Chapter 1

Heavy Neutral Leptons

Neutrino oscillation is the key evidence suggesting that neutrinos have mass, a phenomenon that cannot currently be explained by the Standard Model. An additional right-handed neutral state is required to explain the generation of neutrino mass, constructed via either Dirac or Majorana mass term. Since this new state is much heavier than neutrinos, it is commonly referred to as *Heavy Neutral Leptons* (HNLs).

In Section **??** of this chapter, an overview of HNL as a minimal extension to the Standard Model is presented. Section **??** explains the production mechanism of HNLs from meson decays, enabling HNL searches using charged kaons produced from the Booster Neutrino Beam. Following this, Section **??** details the decay of HNLs into Standard Model observables, such that HNLs decaying in flight can be probed at that Short-Baseline Near Detector. Here, the focus is on the decay channel into a neutrino and a neutral pion, where the neutral pion subsequently decays into two photon showers the detector. Lastly, Section **??** summarises the existing sensitivity limits on the available mixing angle and mass phase space of HNLs through two different experimental methods: peak searches and decay searches.

1.1 HNL Motivation

The phenomenon of three flavour neutrino oscillation is well-established. Active neutrinos are produced and detected as their flavour states ν_μ, ν_e and ν_τ and the neutrino oscillation describes the neutrino flavour states changing from one flavour to another as the neutrinos propagate some distances. Neutrino oscillation directly implies the existence of non-zero mass for at least two out of the three neutrino states. Whilst the Standard Model (SM) of particle physics has proved extremely successful, unfortunately, it currently provides no mechanism for the mass generation of neutrinos. The absence of a right-handed chiral partner to the left-handed chiral neutrino means that no Dirac mass term can be built via the Yukawa coupling of the Higgs to the opposite chirality fields.

This motivates an introduction of a right-handed neutrino such that the neutrino mass can be constructed using the same recipe as all other SM particles. The Dirac mass term in the neutrino Lagrangian after spontaneous symmetry breaking is as follows [1]

$$\mathscr{L}_D = -m_D(\overline{\nu_L}\nu_R + \overline{\nu_R}\nu_L) \tag{1.1}$$

where $m_D = Y v/\sqrt{2}$ is the Dirac mass, Y is the Yukawa coupling, v is the Higgs vacuum expectation value, and the subscript R and L denotes the right and left chiral state of the ν neutrino and $\overline{\nu}$ anti-neutrino field. While the Dirac mass term requires the existence of both left and right-handed chiral states, the Majorana mass term was proposed by Ettore Majorana in 1937 requiring only one chiral state [2]. Under the condition that a particle is its own antiparticle, the charge conjugation operator C can be applied to ν_R such that $\nu_R^C = C\overline{\nu_R}^T$, where the resulting ν_R^C has the correct properties to be used in place of ν_L in Eq. **??** [3]. The construction of the Majorana state violates the charge conservation and is forbidden for any other SM particle with an exception of neutrinos due to their neutral charges. In this case, the Majorana mass term in the neutrino Lagrangian is as follows [3]

$$\mathscr{L}_M = -\frac{1}{2}M(\overline{\nu_R^C}\nu_R + \overline{\nu_R}\nu_R^C) \tag{1.2}$$

where M is the Majorana mass. The factor of a half is introduced to account for double counting since the term $\overline{\nu_R}$ and ν_R^C are not independent.

A right-handed neutral state provides a hypothetical neutrino mass mechanism not only via the Dirac or the Majorana mass term but also via combining both mass terms together. A

generalised Lagrangian in this case is as follows [1]

$$\mathscr{L}_{DM} = -\frac{1}{2}[m_D\overline{\nu_L}\nu_R + m_D\overline{\nu_R^C}\nu_L^C + M\overline{\nu_R^C}\nu_R] + h.c. \tag{1.3}$$

The Lagrangian presented here allows for the seesaw mechanism to construct the physical masses of active neutrinos assuming the Majorana mass term is much larger than the Dirac mass term, $M \gg m_D$ [1, 4]. Under the assumption of only two neutrino states for simplification, the seesaw mechanism would give the mass of a left-handed neutrino state $m_\nu \approx \frac{m_D^2}{M}$ and a right-handed neutrino state $m_N \approx M$, such that the heaviness of m_N suppresses the physical mass of the active neutrino m_ν. Thus, a right-handed heavy neutrino state is a very attractive addition to the SM as an answer to the neutrino mass mechanism, providing an explanation for the extreme lightness of active neutrinos.

The neutral nature of right-handed neutrinos requires all SM charges to be zero implying that they do not interact directly via the strong, electromagnetic, or weak forces. These weaker-than-weak right-handed particles are often referred to as *sterile neutrinos*. The only direct coupling to the new sterile state is neutrino-Higgs interaction. This leads to mixing-mediated interactions with SM gauge bosons, allowing them to be produced and decay via SM gauge interactions with a rate suppressed by the mixing angle [5]. The mass range of sterile neutrinos can span over many orders of magnitudes, and the number of flavour or mass states is unconstrained.

In the mass range of the order $\mathcal{O}(1)$ eV, they are known as *light* sterile neutrinos and proposed to participate in oscillation with active neutrinos. Over a short baseline distance, the addition of a single light sterile neutrino to neutrino oscillation might enhance or reduce the number of observed neutrino interactions for a given channel. Particularly, this model can explain the anomalies observed by the LSND and MiniBooNE experiments, where an excess of ν_e and $\overline{\nu}_e$ interactions was measured at low energy [6].

In the mass range $> \mathcal{O}(10)$ eV, sterile neutrinos are now considered *heavy* since their masses are significantly more massive compared to active neutrinos. This gains them the name *Heavy Neutral Leptons* (HNLs). HNLs do not participate in oscillation with active neutrinos due to coherence loss [5]. As a consequence of being heavier than active neutrinos, the wave packet of HNLs moves much slower compared to that of active neutrinos, and immediately undergoes propagation decoherence. Instead, HNLs are expected to travel over some distances before decaying into SM observables.

Different theoretical models of HNLs have been developed, and a comprehensive review can be found in Ref. [6]. In the search for HNLs presented here, the existence of HNLs will

be explored in a minimal way by assuming an addition of a single HNL to the SM. From a generic phenomenological approach, a HNL can be added to the SM by simply extending the Pontecorvo-Maki-Nakagawa-Sakata (PMNS) matrix. The PMNS matrix, describing the mixing of the SM neutrino flavour eigenstate ν_α ($\alpha = e, \mu, \tau$), and the mass eigenstate ν_i ($i = 1, 2, 3$), is as follows

$$U_{PMNS} = \begin{pmatrix} U_{e1} & U_{e2} & U_{e3} \\ U_{\mu 1} & U_{\mu 2} & U_{\mu 3} \\ U_{\tau 1} & U_{\tau 2} & U_{\tau 3} \end{pmatrix} \tag{1.4}$$

The flavour eigenstate ν_α undergoes weak interaction, whilst the mass eigenstate ν_i describes the neutrino propagation in space and time. For an addition of a single right-handed neutrino with mass m_N, the PMNS matrix can be extended to describe the mass mixing between SM neutrinos and the new flavour eigenstate N as follows

$$U_{PMNS}^{Extended} = \begin{pmatrix} U_{e1} & U_{e2} & U_{e3} & U_{e4} \\ U_{\mu 1} & U_{\mu 2} & U_{\mu 3} & U_{\mu 4} \\ U_{\tau 1} & U_{\tau 2} & U_{\tau 3} & U_{\tau 4} \\ U_{N1} & U_{N2} & U_{N3} & U_{N4} \end{pmatrix} \tag{1.5}$$

where the index 4 is reserved as a new mass eigenstate. Then, the flavour eigenstate ν_α of SM neutrinos can be written as the linear combination of the mass eigenstate ν_i and the HNL flavour eigenstate N as follows

$$\nu_\alpha = \sum_i U_{\alpha i} \nu_i + U_{\alpha 4} N \tag{1.6}$$

where the mixing angles $U_{\alpha i}$ ($\alpha = e, \mu, \tau$ and $i = 1, 2, 3$) are elements of the SM PMNS matrix, and the mixing angle $U_{\alpha 4}$ are the extension. For simplicity, this work only considers a HNL coupling to only one flavour at a time, such that at most one of the three mixing angles U_{e4}, $U_{\mu 4}$ and $U_{\tau 4}$ is non-zero.

1.2 HNL Production

In any SM neutrino production processes, HNLs can be produced in place of neutrinos with a rate suppressed by the mixing angle $|U_{\alpha 4}|^2$, if kinematically allowed. Fig. **??** illustrates the two-body decay of a charged kaon producing a ν_μ and Fig. **??** illustrates the substitution of the ν_μ with a HNL N having $L = +1$ mediated by $|U_{\alpha 4}|^2$. This implies that HNLs can be probed from the Booster Neutrino Beam (BNB), which is an abundance source of mesons

and will be further detailed in Sec. **??**. Since the BNB is primarily made up of positively charged mesons, the following section will focus on the parent meson K^+ and π^+.

(a) **(b)**

Fig. 1.1 Feynman diagrams of (a) $K^+ \to \mu^+ \nu_\mu$ and (b) $K^+ \to \mu^+ N$.

In general, the branching ratio $Br(m^+ \to l_\alpha^+ N)$ of a two-body decay of a charged meson m^+ into a lepton l_α^+ ($\alpha = e, \mu, \tau$) and a HNL N can be expressed in terms of the analogous branching ratio into a SM neutrino as follows [7]

$$Br(m^+ \to l_\alpha^+ N) = Br(m^+ \to l_\alpha^+ \nu_\alpha) \left(\frac{|U_{\alpha 4}|^2}{1 - |U_{\alpha 4}|^2} \right) \rho_N \left(\frac{m_{l_\alpha}^2}{m_{m^+}^2}, \frac{m_N^2}{m_{m^+}^2} \right) \tag{1.7}$$

where $Br(m^+ \to l_\alpha^+ \nu_\alpha)$ is the branching ratio of the charged lepton m^+ decaying into a lepton l_α^+ and a SM neutrino ν_α, m_{m^+} is the mass of the charged meson, m_{l_α} is the mass of the daughter lepton and m_N is the mass of the daughter HNL. The kinematic factor ρ_N accounts for the available phase space of the daughter HNL in the decay and has the complete expansion as follows [7]

$$\rho_N(x, y) = \frac{(x + y - (x - y)^2)\sqrt{1 + x^2 + y^2 - 2(x + y + xy)}}{x(1 - x)^2} \tag{1.8}$$

Fig. **??** depicts the kinematic factor ρ_N of the HNL production compared to the analogous SM neutrino production as a function of the HNL mass. Four HNL production channels that are probable at the BNB are shown: (1) $K^+ \to N e^+$ in the dashed red line, (2) $K^+ \to N \mu^+$ in the solid pink line, (3) $\pi^+ \to N e^+$ in the dashed dark blue line and (4) $\pi^+ \to N \mu^+$ in the solid light blue line. Production channels associated with the τ-flavour mixing angle are not shown since they are kinematically forbidden at the BNB. The kinematic factor for each illustrated channel is constrained by the available mass after the two-body decay of the parent meson, and the upper limit of the HNL mass is $m_N = m_{m^+} - m_{l_\alpha}$ ($\alpha = e, \mu$) as shown by the vertical grey lines. Here it can be seen that the HNL production from π^+ decays limits the HNL mass to < 140 MeV while the HNL production from K^+ decays allows for the

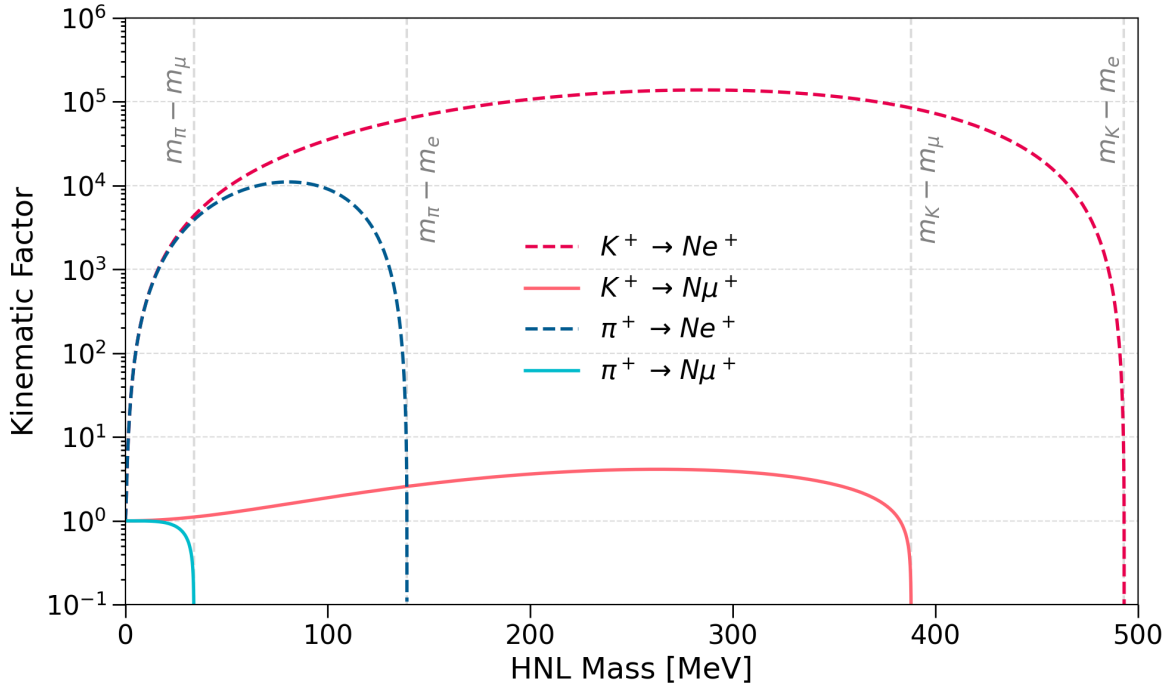

Fig. 1.2 Plot showing the kinematic factor of the HNL production from meson decays as compared to the analogous SM neutrino production.

HNL mass up to 495 MeV. Thus, the search for HNLs presented here focuses on the HNL production channel from K^+ to probe mass as high as 495 MeV.

Furthermore, the magnitude of the kinematic factor of the HNL production shown in Fig. **??** is larger than 1 as compared to the analogous SM production. This is because of the helicity suppression observed in mesons decaying into a SM neutrino having an opposite effect for mesons decaying into a HNL [7]. Instead, it is helicity *enhancement* due to HNLs being massive. For the HNL production channel interested in this work, a significant enhancement is evident for the production rate of $K^+ \to e^+ N$ being increased by a factor of 10^5. On the other hand, the kinematic factor of $K^+ \to \mu^+ N$ unfortunately only peaks at 4, implying a negligible enhancement on the production rate.

1.3 HNL Decay

For HNLs to be detected, they are hypothesised to be able to decay into SM observables [7]. The proposed lifetime of HNLs should be sufficient so that a HNL produced from the BNB must survive long enough to reach the detector and then decay in flight. At the mass range

in the order $\mathcal{O}(100\ \text{MeV})$, the kinematically-allowed decay channels of a HNL produced from the BNB are as follows [5]

$$\begin{aligned} &N \to e^- \pi^+, \quad N \to \mu^- \pi^+, \quad N \to \nu \pi^0, \quad N \to \nu \gamma, \\ &N \to \nu e^- e^+, \quad N \to \nu \mu^- \mu^+, \quad N \to \nu \mu^- e^+, \quad N \to \nu \nu \nu. \end{aligned} \tag{1.9}$$

These decay channels here conserve the lepton number under the assumption that HNLs are Dirac particles with $L = +1$. If HNLs are Majorana particles, such that the lepton number conservation is violated, then the charge conjugates for these decays that would be forbidden in the Dirac case are now allowed.

Fig. **??** depicts branching ratios of decay channels shown in Eq. **??** as a function of HNL mass. Solid lines are branching ratios via the μ-flavour mixing angle ($[U_{e4} : U_{\mu 4} : U_{\tau 4}] = [0 : 1 : 0]$) and dashed lines are branching ratios via the e-flavour mixing angle ($[U_{e4} : U_{\mu 4} : U_{\tau 4}] = [1 : 0 : 0]$). The branching ratios were plotted referencing decay widths from Ref. [5, 8, 9]. Decay widths of HNLs have been derived independently across various literature sources and an overview of discrepancies is summarised in Ref. [9]. The sources used here have been found to be in good agreement with each other.

For $m_N < 135$ MeV, the dominant branching ratio occurs in the channel $N \to \nu\nu\nu$ as shown by the light green lines. However, this channel is almost unobservable since the detection of SM neutrinos relies on the already-small cross section of neutrino scattering with the detector material. The other two channels in this mass range are $N \to \nu e^- e^+$ and $N \to \nu\gamma$, as shown by the light pink and grey lines. The channel $N \to \nu\gamma$ is highly suppressed compared to the channel $N \to \nu e^- e^+$, and thus, the final state of $e^- e^+$ pair provides the best sensitivity within this mass range.

For $m_N > 135$ MeV, a HNL has sufficient mass to decay into either a neutral pion ($m_{\pi^0} = 135$ MeV) or a charged pion ($m_{\pi^+} = 140$ MeV). For the e-flavour mixing angle, the channel $N \to e^- \pi^+$ dominates over the channel $N \to \nu \pi^0$ across the mass range from 135 to 495 MeV, as shown by the dashed dark blue and dashed pink line respectively. In the case of the μ-flavour mixing angle, the leading channel within the mass range of $135 < m_N < 245$ MeV is $N \to \nu \pi^0$ as shown by the solid pink line. Beyond $m_N > 245$ MeV, equivalent to the mass of a muon and a charged pion, the dominant decay channel begins to shift to the channel $N \to \mu^- \pi^+$ as shown by the solid blue light. Finally, both channels $N \to \nu \mu^- e^+$ and $N \to \nu \mu^- \mu^+$ are not competitive compared to any other channels at the same mass value.

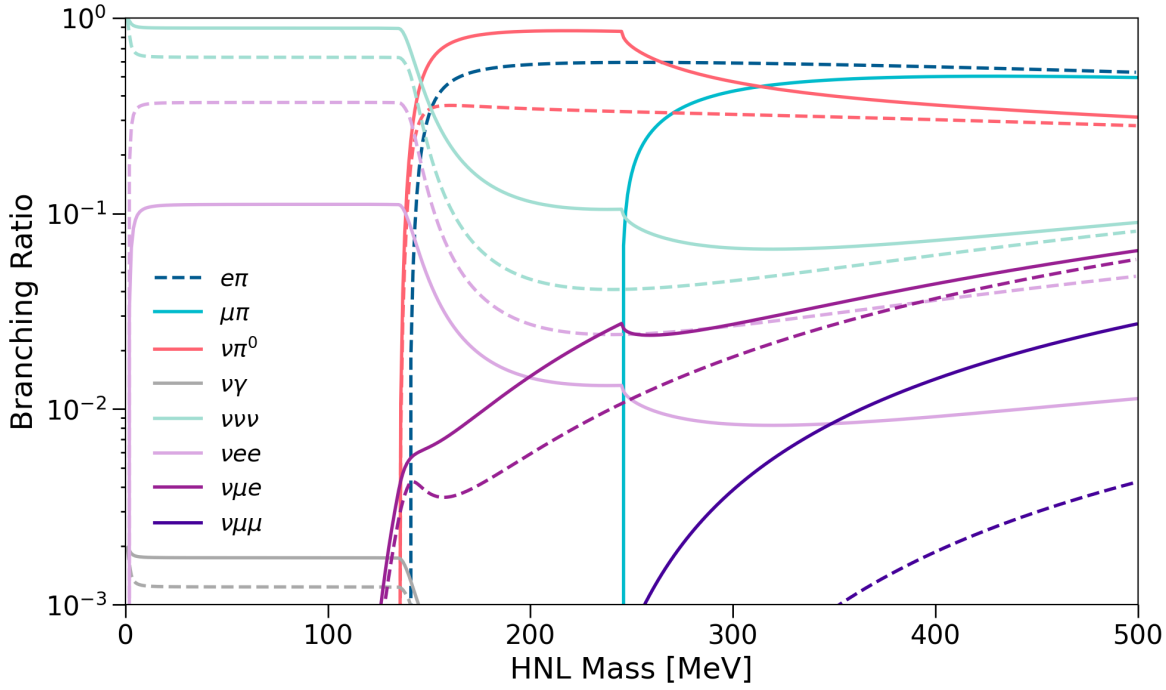

Fig. 1.3 Plot showing the branching ratio of probable decay channels of a HNL produced from the BNB.

Based on the assessment above it was decided in this work to focus on searching for HNLs through the decay channel $N \to \nu\pi^0$, which will be covered in Chapter **??** and **??**. This is the leading channel of the μ-flavour mixing angle within the mass range of $135 < m_N < 245$ MeV. Sensitivity in the same mass range of the e-flavour mixing angle has been extensively explored by many experiments as summarised by Ref. [6]. The decay width for the $N \to \nu\pi^0$ channel as taken from Ref. [9] is as follows

$$\Gamma(N \to \nu\pi^0) = \frac{G_F^2 m_N^3}{32\pi} f_\pi^2 |U_{\mu 4}|^2 \left(1 - \left(\frac{m_{\pi^0}}{m_N}\right)^2\right)^2 \tag{1.10}$$

where G_F is the Fermi constant, f_π is the pion decay constant and m_{π^0} is the mass of a neutral pion. It is noted that the equivalent equations from Ref. [5, 8] contain an additional factor of 2 in the denominator. Eq. **??** was chosen from Ref. [9] since the source is more recently dated.

Fig. **??** shows the diagram of the HNL decaying into the final state $\nu\pi^0$. The SM neutrino is expected to leave no detectable signatures due to their very small scattering cross sections. Meanwhile, the neutral pion is very short-lived with a mean lifetime of $8.52 \pm 0.18 \times 10^{-17}$ s and decays into two photons $98.823 \pm 0.034\%$ of the time [10]. Fig. **??** shows the Feynman

diagram for the described decay. The photon pair results into clear a signature inside a Liquid Argon Time Projection Chamber (LArTPC): two electromagnetic showers without any associated hadronic activities at the decay vertex. This signal topology will face very challenging background separation from some SM neutrino channels also containing a π^0 in the final state. As described in more detail in Chapter **??**, differences in the final state kinematics from the HNL signal to the SM neutrino background enable an effective separation.

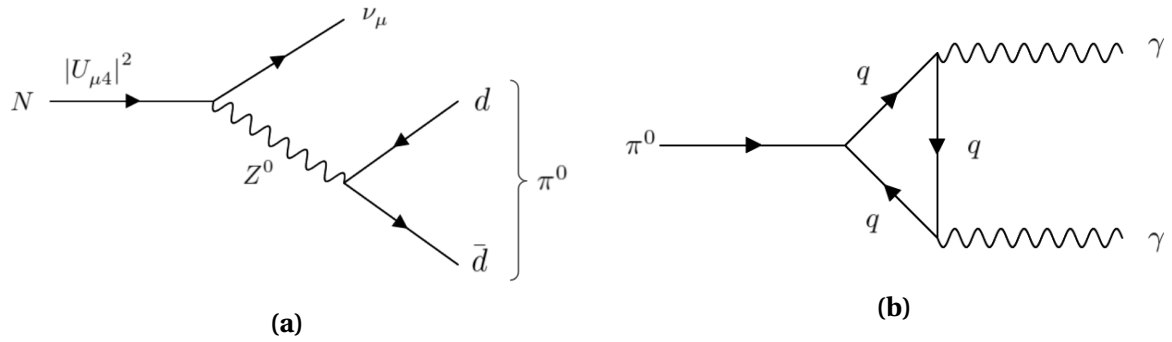

Fig. 1.4 Feynman diagrams of (a) $N \to \nu\pi^0$ mediated by $|U_{\mu 4}|^2$ (b) and $\pi^0 \to \gamma\gamma$.

As discussed in Sec. **??**, HNLs can be either Dirac or Majorana particles in nature. The difference between Dirac and Majorana HNLs is not only the lepton number conservation but also the polarisation of the decay products. In the case of the neutral current final state $\nu\pi^0$, Majorana HNLs decay isotropically, whereas in the case of Dirac HNLs, the angular distribution of the daughter particles is no longer isotropic. The helicity of the daughter neutrino determines the direction of the neutral pion and the angular distribution of the two charge conjugations ($\nu\pi^0$ and $\overline{\nu}\pi^0$) of a Dirac HNL adds up to an isotropic distribution [11]. As the daughter neutrino is undetectable, the observed angular distribution of the neutral pion is expected to be insufficient to determine the Dirac or Majorana nature of HNLs. For simplicity in this search of HNL via the channel $\nu\pi^0$, it is therefore assumed that HNLs are Majorana particles.

1.4 Previous Experimental Searches For HNLs

HNLs have been searched by experiments over the decades, across a wide range of mass. Oscillation experiments and precise β decay experiments have probed HNLs in the mass range between eV and keV, while collider experiments have primarily explored GeV-scale HNLs. To date, no evidence of HNL existence has been found, and thus, experiments have set

upper limits on the coupling $|U_{\alpha 4}|^2$ ($\alpha = e, \mu, \tau$). The sensitivity contour of HNL is commonly expressed in terms of the mixing angle $|U_{\alpha 4}|^2$ as a function of the HNL mass.

Here, current experimental limits on HNLs around $\mathcal{O}$ (100 MeV) are presented, focusing specifically on the mass range of $0 < m_N < 245$ MeV, which is relevant to the final states $\nu\pi^0$. The summary is plotted in Fig. **??**. In this mass range, two key experimental methods are peak searches and decay searches. Peak searches probe only the production rate of HNLs, whereas decay searches probe both production and decay rates.

1.4.1 Peak Searches

Peak search experiments measure the energy spectrum resulting from the decay of meson decay that would produce a HNL. Typically, the two-body leptonic decay of a meson is modelled as $\mathrm{m} \rightarrow l + Missing$, where m is the parent meson (a pion or a kaon) and l is the daughter particle (a pion or a lepton) [12]. The *missing* decay products are attributed to either HNLs or SM neutrinos. HNLs are expected to exit the detector before decaying, whereas SM neutrinos escape the detector before interacting, serving as the primary background for this search. Since the momenta of m and l are precisely measured, the missing invariant mass can therefore be derived as $m^2_{miss} = (P_\mathrm{m} - P_l)^2$, where P_m and P_l are the 4-momentum of the parent and daughter particles. Given the near-zero mass of SM neutrinos, the mass of the daughter HNL can be treated as $m_N = m_{miss}$. Consequently, an excess over the background at m_{miss} would indicate potential existence of HNLs.

To infer the sensitivity contour, the flavour of the daughter lepton determines the flavour of the mixing angle, while the amplitude of the decay spectrum at m_{miss} determines its upper limit. Limits placed by the peak searches are insensitive to the Dirac or Majorana nature of HNLs as it does not impact the kinematics of the meson decay. For the mixing angle $|U_{\mu 4}|^2$, the most competitive limits have been established by the following experiments, particularly on pion and kaon decay spectrum.

Pion Decay Spectrum Peak Searches

- **SIN** (Swiss Institute for Nuclear Research) performed a peak search using stopped positive pions decay via the channel $\pi^+ \rightarrow \mu^+ + Missing$, using a scintillator in 1981 and a germanium detector in 1987. The pion enabled probing HNLs within the low mass range of $\mathcal{O}$(10 MeV). Upper limits of $|U_{\mu 4}|^2$ were placed in the mass range 1–20 MeV at 10^{-4} [13–15].

- The **PIENU** collaboration at TRIUMF also searched for HNLs using stopped pions. The most recent result in 2019 set the most stringent limits on $|U_{\mu 4}|^2$ in the range 10^{-5} in the mass range of 15–34 MeV [16], extending beyond result reported by SIN.

Kaon Decay Spectrum Peak Searches

- The **KEK** collaboration conducted an experiment known as E89, which aimed to search for HNLs using the muon range spectrum resulting from stopped kaon decays during 1981–1982. Following this, experiment E104 in 1983 was carried out with improved momentum resolution and background suppression. The kaons were produced using a 0.5 GeV proton beam, and 3×10^6 muons from kaon decays were analysed using magnetic spectrograph. The outcomes from the E89 experiment constrained the limits of $|U_{\mu 4}|^2$ between 10^{-4}–10^{-6} within the mass range of 70–300 MeV. Additionally, the combined results from the E89 and E104 experiments extended the sensitivity towards the lower mass range between 45–300 MeV, although these findings are currently unpublished [17–19].

- The **E949** collaboration at Brookhaven National Laboratory performed a kaon decay experiment using 21.5 GeV protons in 2002. The analysis on the decays of 2×10^{21} stopped kaons resulted in limits on $|U_{\mu 4}|^2$ within the mass range between 175–300 MeV, constraining at 10^{-7}–10^{-9} [20].

- The **NA62** collaboration, a kaon decay experiment at the CERN super proton synchrotron, analysed 10^8 stopped kaons from 400 GeV protons extracted from the synchrotron. The first results from a data set in 2015 set upper limits on $|U_{\mu 4}|^2$ in the range of 10^{-7}–10^{-6} for HNL masses in the range 250–373 MeV. Updated results using a larger dataset collected in 2016–2018 significantly improved the limits by an order of magnitude to 10^{-8}–10^{-7}, and extended the mass range to 200–384 MeV [21, 22].

1.4.2 Decay Searches

Decay searches look for decay products from HNLs. HNLs are typically produced outside of the detector before reaching it, potentially decaying into SM observables inside the detector. Different combinations of production and decay channels yield different expected event rates, allowing for exploring different sensitivity regions associated with different mixing angles. Decay searches have been historically performed in beam-dump experiments, designed explicitly to suppress background from SM interactions, thereby enabling the

search for rare decay processes. Recently, modern neutrino oscillation experiments with enhanced resolution have emerged as competitive beam-dump experiments alongside their neutrino physics programme. For $|U_{\mu 4}|^2$ within the mass range of 0–245 MeV, the most competitive limits have been set by the following experiments.

- The CERN **PS191** experiment in 1984 utilised an exposure of 19.2 GeV protons on a beryllium target, generating 10^{19} Proton On Target (POT). The detector was positioned at 128 m from the target at an off-axis angle of 2.3° with respect to the beam direction. It was designed specifically to search for HNLs by maximising the signal rate while minimising the background rate. The 216 m^3 volume (12 m long and a cross-sectional area of 18 m^2) was filled with helium. The sparse medium was chosen to reduce background rates arising from SM neutrino interactions, leveraging the large volume to provide a high rate of HNL signals. Limits on $|U_{\mu 4}|^2$ within the mass range of 120–350 MeV were placed in the range of 10^{-5}–10^{-9} [23, 24]. A re-evaluation in 2022 found the limits to be lower than the original published results [25].

- The **NuTeV** collaboration at Fermilab conducted HNLs searches in 1996 using a high energy neutrino beam produced by protons accelerated from the Tevatron ring. The dataset comprised of an exposure of 3×10^{18} POT with an energy of 800 GeV. HNLs were produced from the D mesons resulting from proton collisions with the target. This enabled exploration of HNL masses up to 2000 MeV, surpassing any other beam-dump experiments described here. The experiment established limits on $|U_{\mu 4}|^2$ in the range 10^{-6}–10^{-7} within the mass range of 225–2000 MeV [26].

- The **MicroBooNE** collaboration conducted a series of searches for HNLs using a LArTPC, beginning with the first result in 2020 and subsequent results in 2022 and 2023. The initial analysis was performed using an exposure of 2×10^{20} POT obtained from the on-axis BNB. A special delayed trigger was implemented to identify HNLs arriving at the detector later than SM neutrinos. Limits on $|U_{\mu 4}|^2$ were set in the range of 10^{-7} for HNL masses spanning between 260–385 MeV. The latter two searches focused on HNLs arising from kaons decays in the NuMI absorber, which arrived at the detector at an angle to SM neutrinos from the BNB. The dataset comprised of two runs with an exposure of 2×10^{20} and 5.01×10^{20} POT. The combined results incorporated multiple HNL decay channels, probing a wide mass spectrum between 10–385 MeV. Notably, these recent results have set the most stringent limits to date on $|U_{\mu 4}|^2$, ranging between in the range 10^{-4}–10^{-7} within the mass range of 34–175 MeV, thus extending the findings from 2019 [27–29].

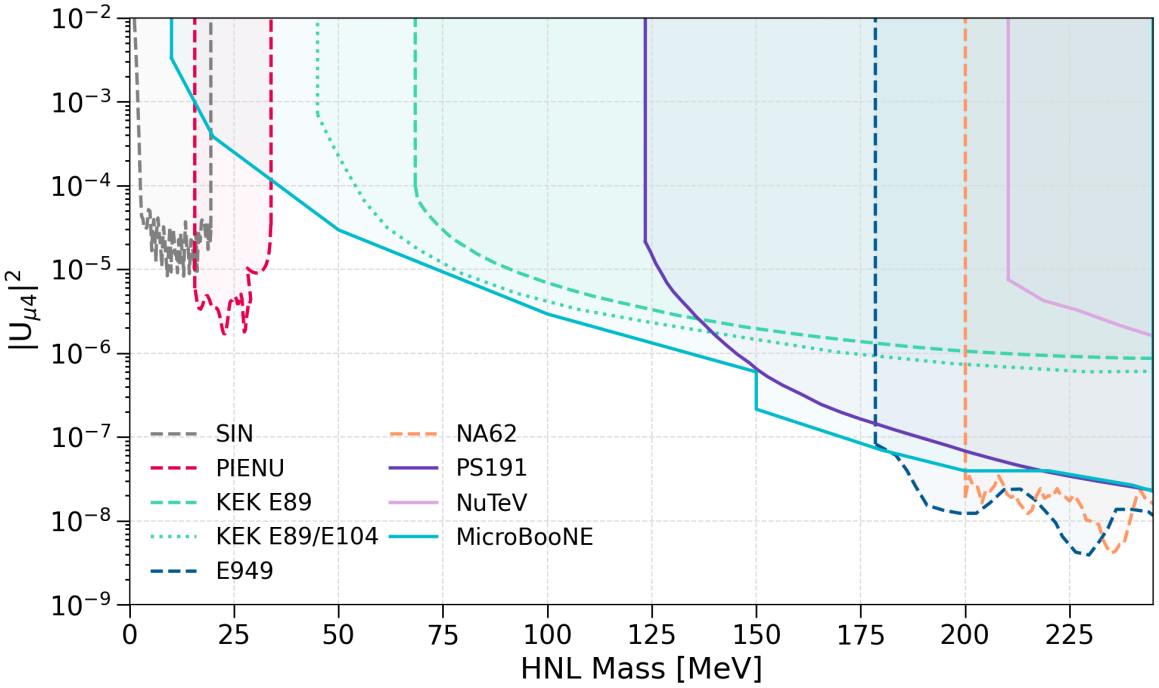

Fig. 1.5 Sensitivity contour of the upper limits on the mixing angle $|U_{\mu 4}|^2$ for Majorana HNLs, within the mass range of $0 < m_N < 245$ MeV. Dashed lines show the constraints derived from peak searches, whilst solid lines show the limits set by decay searches. The dotted line shows the unpublished limit from the KEK E89/E104 experiments.

1.5 Concluding Remarks

HNLs are BSM particles that provide a natural explanation not just for the mass generation of active neutrinos but also for their extreme lightness. The SBND, located only 110 m from the BNB, is capable of detecting HNLs coming from meson decays in the beam, which then decay in flight inside the detector. Novel light detection and reconstruction techniques, resulting in precise timing resolution, enables the separation of HNL signals from SM neutrino backgrounds (See Chapter **??**). Here, the focus is on the $\nu\pi^0$ final state, distinctive event topology featuring two forward-going photon showers without any hadronic activities at the shared vertex. In the mass range between $135 < m_N < 245$ MeV of the mixing angle $|U_{\mu 4}|^2$, the sensitivity is relatively unexplored. This presents a compelling opportunity for SBND to set competitive limits in this region.

References

[1] M. Thomson, *Modern particle physics* (Cambridge University Press, New York, 2013).

[2] E. Majorana, "Teoria simmetrica dell'elettrone e del positrone", Nuovo Cim. **14**, 171–184 (1937).

[3] C. Giunti et al., *Fundamentals of Neutrino Physics and Astrophysics* (Oxford University Press, Incorporated, 2007).

[4] S. F. King, "Neutrino mass models", Rept. Prog. Phys. **67**, 107–158 (2004).

[5] P. Ballett et al., "MeV-scale sterile neutrino decays at the Fermilab Short-Baseline Neutrino program", JHEP **04**, 102 (2017).

[6] M. A. Acero et al., "White Paper on Light Sterile Neutrino Searches and Related Phenomenology", (2022).

[7] J. M. Berryman et al., "Searches for Decays of New Particles in the DUNE Multi-Purpose Near Detector", JHEP **02**, 174 (2020).

[8] A. Atre et al., "The Search for Heavy Majorana Neutrinos", JHEP **05**, 030 (2009).

[9] P. Coloma et al., "GeV-scale neutrinos: interactions with mesons and DUNE sensitivity", Eur. Phys. J. C **81**, 78 (2021).

[10] P. A. Zyla et al. (Particle Data Group), "Review of Particle Physics", PTEP **2020**, 083C01 (2020).

[11] P. Ballett et al., "Heavy Neutral Leptons from low-scale seesaws at the DUNE Near Detector", JHEP **03**, 111 (2020).

[12] O. Goodwin, "Search for Higgs Portal Scalars and Heavy Neutral Leptons Decaying in the MicroBooNE Detector", PhD thesis (The University of Manchester, 2022).

[13] R. Abela et al., "Search for an Admixture of Heavy Neutrino in Pion Decay", Phys. Lett. B **105**, [Erratum: Phys.Lett.B 106, 513 (1981)], 263–266 (1981).

[14] R. C. Minehart et al., "Search for Admixtures of Massive Neutrinos in the Decay $\pi^+ \to \mu^+ + \overline{\nu}$", Phys. Rev. Lett. **52**, 804–807 (1984).

[15] M. Daum et al., "Search for admixtures of massive neutrinos in the decay $\pi^+ \to \mu^+ + \nu$", Phys. Rev. D **36**, 2624–2632 (1987).

[16] A. Aguilar-Arevalo et al. (PIENU), "Search for heavy neutrinos in $\pi \to \mu\nu$ decay", Phys. Lett. B **798**, 134980 (2019).

[17] Y. Asano et al., "Search for a Heavy Neutrino Emitted in $K^+ \to \mu^+$ Neutrino Decay", Phys. Lett. B **104**, 84–88 (1981).

[18] R. S. Hayano et al., "Heavy-Neutrino Search Using $K_{\mu 2}$ Decay", Phys. Rev. Lett. **49**, 1305–1309 (1982).

[19] T. Yamazaki et al., "Search for Heavy Neutrinos in Kaon Decay", in Proc. of the 22nd International Conference on High Energy Physics, Vol. 840719, edited by A. Meyer et al. (1984), p. 262.

[20] A. V. Artamonov et al. (E949), "Search for heavy neutrinos in $K^+ \to \mu^+ \nu_H$ decays", Phys. Rev. D **91**, [Erratum: Phys.Rev.D 91, 059903 (2015)], 052001 (2015).

[21] E. Cortina Gil et al. (NA62), "Search for heavy neutral lepton production in K^+ decays", Phys. Lett. B **778**, 137–145 (2018).

[22] E. Cortina Gil et al. (NA62), "Search for K^+ decays to a muon and invisible particles", Phys. Lett. B **816**, 136259 (2021).

[23] G. Bernardi et al., "Search for neutrino decay", Physics Letters B **166**, 479–483 (1986).

[24] G. Bernardi et al., "Further limits on heavy neutrino couplings", Physics Letters B **203**, 332–334 (1988).

[25] C. A. Argüelles et al., "Heavy neutral leptons below the kaon mass at hodoscopic neutrino detectors", Phys. Rev. D **105**, 095006 (2022).

[26] A. Vaitaitis et al. (NuTeV, E815), "Search for neutral heavy leptons in a high-energy neutrino beam", Phys. Rev. Lett. **83**, 4943–4946 (1999).

[27] P. Abratenko et al. (MicroBooNE), "Search for Heavy Neutral Leptons Decaying into Muon-Pion Pairs in the MicroBooNE Detector", Phys. Rev. D **101**, 052001 (2020).

[28] P. Abratenko et al. (MicroBooNE), "Search for long-lived heavy neutral leptons and Higgs portal scalars decaying in the MicroBooNE detector", Phys. Rev. D **106**, 092006 (2022).

[29] P. Abratenko et al. (MicroBooNE), "Search for heavy neutral leptons in electron-positron and neutral-pion final states with the MicroBooNE detector", (2023).